Interferometric Fourier transform coherent anti-stokes Raman scattering

M. Cui, Manuel Joffre, J. Skodack, Jennifer Ogilvie

Interferometric Fourier transform coherent anti-stokes Raman scattering

Meng Cui

Department of Physics, University of Michigan, Ann Arbor, MI 48109
mcui@umich.edu

Manuel Joffre

Laboratoire d'Optique et Biosciences, Centre National de la Recherche Scientifique Unité Mixte de Recherche 7645 – Institut National de la Santé et de la Recherche Médicale U696 – Ecole Polytechnique, 91128 Palaiseau, France.
manuel.joffre@polytechnique.fr

Joshua Skodack, Jennifer P. Ogilvie

Department of Physics and the Biophysics Research Division, University of Michigan, Ann Arbor, MI 48109
joshsko@umich.edu, jogilvie@umich.edu

Abstract: We present an interferometric time-domain Fourier transform implementation of coherent anti-Stokes Raman scattering (CARS). Based on a single femtosecond laser source, the method provides a straight-forward scheme for obtaining high resolution CARS spectra. We give a theoretical description of the method, and demonstrate good agreement between simulation and experimental CARS spectra. We also discuss the method's relation to other CARS approaches for microscopy and microspectroscopy applications.

OCIS codes: (300.6230) Spectroscopy, coherent anti-Stokes Raman scattering; (190.4810) Multiphoton processes; (170.6920) Time-resolved imaging

References and links

1. A. Zumbusch, G. R. Holtom, and X. S. Xie, "Three-dimensional vibrational imaging by coherent anti-Stokes Raman scattering," Phys. Rev. Lett. **82**, 4142-4145 (1999).
2. J. X. Cheng, and X. S. Xie, "Coherent anti-Stokes Raman scattering microscopy: Instrumentation, theory, and applications," J. Phys. Chem. B **108**, 827-840 (2004).
3. J. P. Ogilvie, E. Beaurepaire, A. Alexandrou, and M. Joffre, "Fourier-transform coherent anti-Stokes Raman scattering microscopy," Opt. Lett. **31**, 480-482 (2006).
4. M. D. Duncan, J. Reintjes, and T. J. Manuccia, "Scanning coherent anti-Stokes Raman microscope," Opt. Lett. **7**, 350-352(1982).
5. M. Muller, and J. M. Schins, "Imaging the thermodynamic state of lipid membranes with multiplex CARS microscopy," J. Phys. Chem. B **106**, 3715-3723 (2002).
6. J. X. Chen, A. Volkmer, L. D. Book, and X. S. Xie, "Multiplex coherent anti-Stokes Raman scattering microspectroscopy and study of lipid vesicles," J. Phys. Chem. B **106**, 8493-8498 (2002).
7. S. Roy, T. R. Meyer, and J. R. Gord, "Broadband coherent anti-Stokes Raman scattering spectroscopy of nitrogen using a picosecond modeless dye laser," Opt. Lett. **30**, 3222-3224 (2005).
8. N. Dudovich, and D. Oron, Y. Silberberg, "Single-pulse coherently controlled nonlinear Raman spectroscopy and microscopy," Nature **418**, 512-514 (2002).
9. N. Dudovich, D. Oron, and Y. Silberberg, "Single-pulse coherent anti-Stokes Raman spectroscopy in the fingerprint spectral region," J. Chem. Phys. **118**, 9208-9215 (2003).
10. J. X. Cheng, A. Volkmer, L. D. Book, and X. S. Xie, "An epi-detected coherent anti-Stokes Raman scattering (e-CARS) microscope with high spectral resolution and high sensitivity," J. Phys. Chem. B **105**, 1277-1280 (2001).
11. Y. X. Yan, and K. A. Nelson, "Impulsive stimulated light-scattering. 2. Comparison to frequency-domain light-scattering spectroscopy," J. Chem. Phys. **87**, 6257-6265 (1987).

#72524 - $15.00 USD Received 30 June 2006; revised 21 August 2006; accepted 24 August 2006

12. A. M. Weiner, D. E. Leaird, G. P. Wiederrecht, and K. A. Nelson, "Femtosecond multi-pulse impulsive stimulated Raman-scattering spectroscopy," J. Opt. Soc. Am. B **8**, 1264-1275 (1991).
13. S.-H. Lim, A. G. Caster, and S. R. Leone, "Single-pulse phase-control interferometric coherent anti-Stokes Raman scattering spectroscopy," Phys. Rev. A **72**, 041803R (2005).
14. S. H. Lim, A. G. Caster, O. Nicolet, and S. R. Leone, "Chemical imaging by single pulse interferometric coherent anti-Stokes Raman scattering microscopy," J. Phys. Chem. B **110**, 5196-5204 (2006).
15. K. P. Knutsen, J. C. Johnson, A. E. Miller, P. B. Petersen, and R. J. Saykally, "High spectral resolution multiplex CARS spectroscopy using chirped pulses," Chem. Phys. Lett. **387**, 436-441 (2004).
16. T. Hellerer, A. M. K. Enejder, and A. Zumbusch, "Spectral focusing: High spectral resolution spectroscopy with broad-bandwidth laser pulses," Appl. Phys. Lett. **85**, 25-27 (2004).
17. B. Yellampalle, R. D. Averitt, A. Efimov, and A. J. Taylor, "Spectral interferometric coherent Raman imaging," Optics Express **13**, 7672-7682 (2005).
18. R. Porter, F. Shan, and T. Guo, "Coherent anti-Stokes Raman scattering microscopy with spectrally tailored ultrafast pulses," Rev. Sci. Instrum. **76**, 043108 (2005).
19. H. N. Paulsen, K. M. Hilligsoe, J. Thogersen, S. R. Keiding, and J. J. Larsen, "Coherent anti-Stokes Raman scattering microscopy with a photonic crystal fiber based light source," Opt. Lett. **28**, 1123-1125 (2003).
20. T. W. Kee, and M. T. Cicerone, "Simple approach to one-laser, broadband coherent anti-Stokes Raman scattering microscopy," Opt. Lett. **29**, 2701-2703 (2004).
21. R. Merlin: "Generating coherent ths phonons with light pulses," Solid State Commun. **102**, 207-220 (1997).
22. A. Volkmer, L. D. Book, and X. S. Xie, "Time-resolved coherent anti-Stokes Raman scattering microscopy: Imaging based on Raman free induction decay," Appl. Phys. Lett. **80**, 1505-1507 (2002).
23. M. Greve, B. Bodermann, H. R. Telle, P. Baum, and E. Riedle, "High-contrast chemical imaging with gated heterodyne coherent anti-Stokes Raman scattering microscopy," Appl. Phys. B **81**, 875-879 (2005).
24. D. L. Marks, C. Vinegoni, J. S. Bredfeldt, and S. A. Boppart, "Interferometric differentiation between resonant and coherent anti-Stokes Raman scattering and nonresonant four-wave-mixing processes," Appl. Phys. Lett. **85**, 5787-5789 (2004).
25. S. Roy, T. R. Meyer, and J. R. Gord, "Time-resolved dynamics of resonant and nonresonant broadband picosecond coherent anti-Stokes Raman scattering signals," Appl. Phys. Lett. **87**, 264103 (2005).
26. M. D. Levenson, and G. L. Eesley, "Polarization-selective optical heterodyne detection for dramatically improved sensitivity in laser spectroscopy," Appl. Phys. **19**, 1(1979).
27. E. O. Potma, C. L. Evans, and X. S. Xie, "Heterodyne coherent anti-Stokes Raman scattering (CARS) imaging," Opt. Lett. **31**, 241-243 (2006).
28. D. Oron, N. Dudovich, and Y. Silberberg, "Single-pulse phase-contrast nonlinear Raman spectroscopy," Phys. Rev. Lett. **89,** 273001 (2002).
29. G. W. Jones, D. L. Marks, C. Vinegoni, and S. A. Boppart, "High-spectral-resolution coherent anti-Stokes Raman scatterind with interferometrically detected broadband chirped pulses," Opt. Lett. **31**, 1543-1545 (2006).
30. C. L. Evans, E. O. Potma, and X. S. Xie, "Coherent anti-Stokes Raman scattering spectral interferometry: Determination of the real and imaginary components of nonlinear susceptibility $\chi^{(3)}$ for vibrational microscopy," Opt. Lett. **29**, 2923-2925 (2004).
31. Sadtler: *The Sadtler standard Raman spectra*. Philadelphia: Sadtler Research Laboratories, subsidiary of Block Engineering; 1973.
32. E. Frumker, E. Tal, Y. Silberberg, and D. Majer, "Femtosecond pulse-shape modulation at nanosecond rates," Opt. Lett. **30**, 2796-2798 (2005).

1. Introduction

The promise of detailed chemical information based on endogenous contrast has generated much recent interest in coherent anti-Stokes Raman scattering (CARS) microscopy. Due to its nonlinear nature, CARS microscopy shares the benefits of multiphoton microscopy, such as automatic sectioning and enhanced depth penetration, while avoiding problems associated with fluorescent labeling [1,2]. In this paper we discuss a Fourier transform-based CARS (FTCARS) method that we recently demonstrated to provide high resolution spectrally-resolved CARS images [3]. The technique employs a single broadband laser source and provides a simple approach to CARS microscopy and microspectroscopy. Here we discuss in detail the origin of the FTCARS signal, and compare FTCARS to other CARS schemes currently being employed. We also demonstrate interferometric amplification of the FTCARS signal, providing two orders of magnitude enhancement of the signal.

CARS is a nonlinear scattering process in which light of different frequencies interacts through the third order susceptibility of the medium. As depicted in Fig. 1(a), CARS involves

#72524 - $15.00 USD Received 30 June 2006; revised 21 August 2006; accepted 24 August 2006

four fields: a pump field at frequency ω_p and Stokes field at frequency ω_s create a Raman coherence in the medium. A third field at frequency ω_{pr} probes this coherence to create a higher energy anti-Stokes field at frequency ω_{as}. As well as the resonant CARS process, other possible nonresonant interactions such as those shown in Fig. 1(b) may also occur, giving rise to a "nonresonant background". Since its first demonstration in 1982 [4], the nonresonant background has been a common problem that has plagued CARS microscopy. Recent implementations of CARS have employed narrowband near-infrared lasers and polarization selection to limit its effects [2].

While reducing the nonresonant background and efficiently exciting specific CARS modes, the use of picosecond excitation restricts the spectral range of the CARS measurement: images taken with this approach typically map a single vibration. Providing

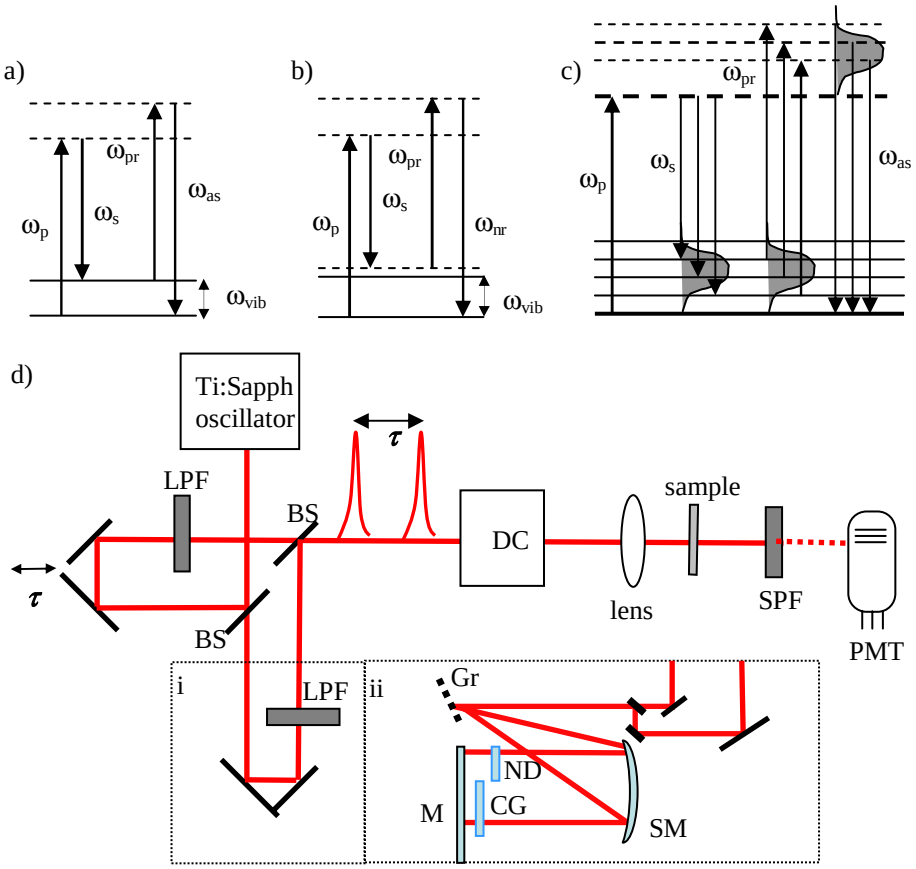

Fig. 1. (a). Resonant CARS process. (b) Nonresonant CARS process. (c) Multiplex CARS – multiple Raman coherences can be generated when broadband Stokes light is available. (d) (i) Experimental implementation of standard FTCARS. BS: beamsplitter, DC: dispersion compensation (chirped mirrors), LPF: long pass filter, SPF: short pass filter, PMT: photomultiplier tube. (ii) Experimental setup for Homodyne CARS. Gr: 600 lines/mm grating, ND: neutral density filter, CG: compensating glass, M: mirror, SM: spherical mirror (f=30 cm).

access to the entire fingerprint spectral region, where CARS spectra are most distinct, would enable high chemical resolution and the simultaneous imaging of multiple chemical species, thereby significantly enhancing the capabilities of CARS microscopy. CARS methods employing picosecond excitation can obtain broadband CARS images by the time-consuming

#72524 - $15.00 USD Received 30 June 2006; revised 21 August 2006; accepted 24 August 2006

process of tuning one of the excitation frequencies [2]. A more practical approach has been "multiplex CARS", which combines narrowband picosecond and femtosecond excitation to obtain CARS images with ~200 cm^{-1} of bandwidth [5,6]. In this approach, the narrowband "pump" pulse provides relatively high spectral resolution, while the broadband "Stokes" pulse provides access to multiple CARS modes within its spectral bandwidth, as depicted in Fig. 1(c). A similar multiplex approach has recently been used in CARS spectroscopy applications, to obtain spectra with bandwidths of ~140 cm^{-1}[7].

With a pulse as short as 10 fs, the entire fingerprint region (~1500 cm^{-1}) can be accessed, as demonstrated recently by Silberberg *et al*. [8, 9]. Rather than mixing picosecond and femtosecond excitation, the Silberberg group employed a single femtosecond laser, obviating the need for the active synchronization methods that are required when multiple laser sources are used [10]. This approach is analogous to impulsive stimulated Raman scattering (ISRS) [11], where a single short pulse simultaneously excites all Raman modes within the laser bandwidth. Similar to previous ISRS work [12], Silberberg *et al*. obtained spectral selectivity via pulse-shaping techniques, which also greatly reduced the nonresonant background that represents a greater problem for shorter pulses [10]. Following the work of the Silberberg group [8,9], a number of groups have implemented CARS schemes employing single femtosecond laser sources. These methods either excite specific CARS modes, or achieve enhanced spectral resolution by techniques such as phase and polarization pulse-shaping [13,14], spectral focusing with chirped pulses [15-17], or amplitude shaping of pump and Stokes pulses.[18] Other recent implementations of CARS have combined narrowband pump with broadband Stokes excitation obtained by spectral broadening in a tapered or photonic crystal fiber [19,20].

We recently demonstrated a simple time-domain Fourier transform method for CARS microscopy [3]. The method employs a single femtosecond laser, and is similar in principle to Silberberg's implementation, which used phase-shaping to convert a single femtosecond pulse into a train of subpulses spaced by an appropriate quasi-period to excite specific CARS modes. In Silberberg's implementation, a CARS spectrum can be obtained by recording the CARS signal as a function of the quasi-period applied by the pulse-shaper. Rather than obtaining the CARS spectrum by alternately exciting specific CARS modes, the complete CARS spectrum can be obtained through the Fourier transform of time-domain ISRS data [12]. Our method employs this approach, with the benefits of ease of implementation, high spectral resolution over the full fingerprint region and easy suppression of the nonresonant background. Fourier transform CARS (FTCARS) relies on the same physical principles as ISRS [11, 21], but employs a geometry and signal detection scheme more appropriate for applications in microscopy: the desire for rapid signal detection precludes the use of lock-in detection, while a desire for high spatial resolution motivates the use of a collinear geometry. Here we present a description of the technique, which differs from previous descriptions of ISRS in the geometry and the signal detection method.

2. Theoretical description of FTCARS

In FTCARS a sequence of pump and probe broadband femtosecond pulses is incident upon the sample. As in ISRS, the pump, or "excitation" pulse, generates Raman coherences in all modes within the pulse bandwidth, while the second pulse probes the coherences. Both Stokes and anti-Stokes fields are generated, and the anti-Stokes field is selected via spectral filtering. A long-pass filter located before the sample provides a sharp cut on the blue edge of the spectrum, while a short-pass filter separates the blue-shifted anti-Stokes signal from the incident pump and probe light [see Fig. 1(d)]. The anti-Stokes signal is then recorded as a function of the time delay between the pump and probe pulses. The nonresonant background generated by combined pump and probe interactions can be windowed out, allowing retrieval of the CARS spectrum upon Fourier transform. As with any Fourier transform technique, the spectral resolution of the FTCARS measurement depends on the maximum time delay,

#72524 - $15.00 USD Received 30 June 2006; revised 21 August 2006; accepted 24 August 2006

providing the capability of achieving high spectral resolution.The idea that resonant and nonresonant signals have different temporal responses has been employed in CARS experiments at fixed time delays [22, 23], and an interferometric CARS experiment of a single CARS mode [24]. It has also been used recently in frequency-domain CARS spectroscopy applications.[7, 25]

The generation of the FTCARS signal can be understood by considering the third order polarization driving it. Following the treatment of Dudovich et al., third order perturbation theory describes the resonant polarization $P_R^{(3)}(\omega)$ created by a single femtosecond pulse with electric field envelope *E(ω)* as: [9]

$$P_R^{(3)}(\omega) \propto \int_0^\infty d\Omega \frac{1}{\Omega - \Omega_R - i\Gamma_R} E(\omega - \Omega) A(\Omega) \tag{1}$$

where

$$A(\Omega) = \int_0^\infty d\omega' E^*(\omega') E(\Omega + \omega') \tag{2}$$

describes all possible two photon pairs leading to the same intermediate state and Ω_R and Γ_R are the Raman frequency and linewidth. Similarly, the nonresonant polarization is given by:[9]

$$P_{NR}^{(3)}(\omega) \propto \int_0^\infty \frac{d\Omega}{\Omega} E(\omega - \Omega) A(\Omega) \tag{3}$$

Here the factor $1/\Omega$ has been introduced to account for the fact that the finite pulsewidth leading to a noninstantaneous response.[9] Our applied electric field is the sum of pump and probe pulses with a time delay τ: $E(\tau, t) = E_{pump}(t) + E_{probe}(t - \tau)$. Since spectral filtering is necessary to isolate the CARS signal in a collinear geometry, the pump and probe fields here have both been modified by a long pass filter. This filter serves to provide a sharp blue edge to the spectrum to allow for effective filtering of the CARS signal by a short pass filter located just before the detector. While the spectral filtering scheme removes light that has not been blue-shifted, both the resonant CARS and nonresonant polarizations will have blue-shifted components. Thus the total FTCARS signal is detected in the time domain as:

$$S_{FTCARS}(\tau) \propto \int_0^\infty \left| P_{FTCARS}(\tau, t) \right|^2 dt \tag{4}$$

where

$$P_{FTCARS}(\tau, t) = P_R^{(3)}(\tau, t) + P_{NR}^{(3)}(\tau, t) \tag{5}$$

and $P_R^{(3)}(\tau, t)$ and $P_{NR}^{(3)}(\tau, t)$ are the Fourier transforms of $P_R^{(3)}(\omega)$ and $P_{NR}^{(3)}(\omega)$ computed from the delay dependent electric field $E(\tau, t)$ and spectrally modified by the short pass filter.

In FTCARS there are a number of different signals to consider. Because both pump and probe pulses provide impulsive excitation, they individually produce both resonant and nonresonant polarizations. However, only those signals requiring both pump and probe fields will appear as oscillations in the time domain FTCARS data: contributions solely from the pump or probe pulse will produce a constant background signal. At short delays there are several combinations of pump and probe fields that will give rise to resonant and nonresonant signals. However, when the pump and probe are well-separated, (but before the decay of the Raman mode) a resonant contribution is produced by two pump field interactions that act to create the Raman coherence, and a single probe field interaction. The only other contributions (resonant and nonresonant) that are time-coincident on the detector come solely from the probe pulse and therefore have a third order dependence on the probe field. These probe contributions do not depend on the time delay, but mix with the resonant signal produced by pump and probe pulses.

#72524 - $15.00 USD Received 30 June 2006; revised 21 August 2006; accepted 24 August 2006

More explicitly the polarization components giving rise to the oscillatory FTCARS signal are given by

$$P_{FTCARS}(\tau) \approx P_R^{both}(\tau) + P_{NR}^{both}(\tau) + P_R^{probe} + P_{NR}^{probe} \quad (6)$$

where $P_R^{both}(\tau)$ and $P_{NR}^{both}(\tau)$ refer to the respective resonant and nonresonant CARS polarizations generated by the combination of both pump and probe pulses. Similarly, P_R^{probe} and P_{NR}^{probe} are the respective resonant and nonresonant CARS polarizations generated by the probe pulse alone; we have neglected the contributions arising solely from the pump pulse because these are not time-coincident with the other components. The explicit field dependence of the components is given by:

$$P_{FTCARS} \approx \chi_R^{(3)} I_{pump} E_{probe} + \chi_R^{(3)} I_{probe} E_{probe} + \chi_{NR}^{(3)} I_{probe} E_{probe} \quad (7)$$

Upon homodyne mixing between the CARS emission due to the probe alone and the resonant CARS emission due to both pump and probe, the detected signal (given by Eq. 4) produces terms with the following power dependence:

$$S_{FTCARS} \approx \chi_R^{(3)} I_{pump} I_{probe}^2 \quad (8)$$

The other signal contributions produce low frequency components following Fourier transformation of the windowed FTCARS data.

The mixing of a desired signal with a "local oscillator" (LO) is a frequently used method of signal enhancement termed homodyne detection[26]. In homodyne detection, the optimization of the relative amplitude and phase of the LO can provide orders of magnitude enhancement in detection sensitivity, and provide the ability to separate quadrature components of the signal field. Several groups have previously demonstrated homodyne detection for CARS microscopy applications.[13,14,23,27-30] While the FTCARS signal is the sum of several contributions, control over their relative amplitudes and phase to enhance the resonant FTCARS signal is not readily available. A LO for FTCARS must be time-coincident, and contain frequencies appropriate to interfere with the blue-shifted resonant signal. The broad bandwidth of our probe pulse suggests that the blue edge of the spectrum, which is normally attenuated by a long pass filter to enable effective separation of the FTCARS signal could be used for homodyne detection. We implement this method as shown in the inset of Fig. 1(d) version (ii). We note that this homodyne arrangement has excellent passive phase stability since the LO is derived from the probe pulse itself: any phase drift will be common to both signal and local oscillator and will not affect their relative phase.

3. Experimental implementation

We implemented FTCARS spectroscopy using a broadband Ti:sapphire oscillator (Femtolasers Synergy). Before reaching the sample, the 75 MHz pulse train was sent into a Michelson interferometer, producing two collinear pulses that could be variably time-delayed with respect to each other as shown in Fig. 1(d), version (i). Dispersion precompensation was performed with chirped mirrors, which was optimized via second-order autocorrelations in a GaAsP two-photon photodiode at the sample position to achieve 17 fs pulses. The pump and probe pulses were focused with a 5 cm lens to a spot size of ~30 μm at the sample. The CARS signal was isolated by spectral filtering, which was achieved by a combination of a long pass filter (Omega, cutoff 740 nm) placed before the sample, and two short pass filters (Omega, cutoff 720 nm) located before the detection PMT (Hamamatsu R928). The analog time-resolved CARS signal was digitized at 1 MHz (National Instruments, PCI-6110E). Subsequent data processing to remove the nonresonant background was performed using LabView 7.0 (National Instruments).

#72524 - $15.00 USD Received 30 June 2006; revised 21 August 2006; accepted 24 August 2006

For interferometric detection we modified the setup as shown in the inset of Fig. 1(d), version ii). While the pump spectrum was still sharply cut by the long pass filter at 740 nm, the probe was sent into a zero dispersion stretcher, where a variable neutral density (ND) filter inserted at the Fourier plane allowed control over the amplitude of wavelengths below 740 nm to provide a local oscillator for mixing with the blue-shifted CARS signal. Equal amounts of glass were inserted both into the remaining part of the spectrum at the Fourier plane, and into the pump arm to maintain ~transform-limited (17 fs) pump and probe pulses. Rotation of a glass compensating slide allowed control over the relative phase of the local oscillator field and the resonant and nonresonant CARS signals.

4. Comparison of simulated and experimental results

From Eq. (4) we calculate the FTCARS signal for pyridine which has two dominant CARS modes at 990 cm^{-1} and 1030 cm^{-1}, with smaller peaks at 983 cm^{-1} and 1070 cm^{-1} [31] and compare this to experimental FTCARS data. Figure 2(a) shows the spectra of the pump and probe pulses used in the calculations (left) and experiment (right), along with the locations of the long and short pass filters used to isolate the CARS signal. The computed and measured time domain FTCARS signals are shown in Fig. 2(b), with an inset to provide a more detailed

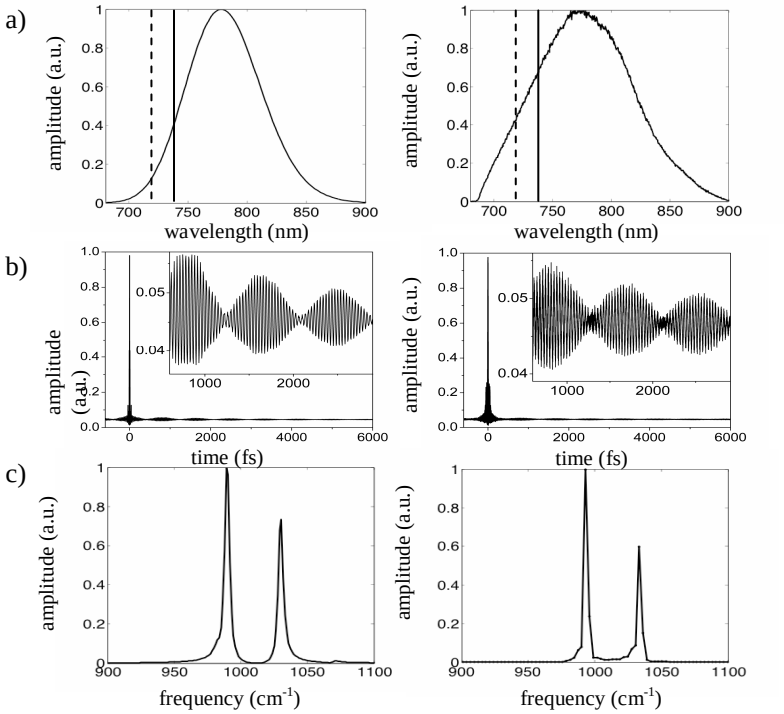

Fig. 2. Simulated (left) and experimental (right) FTCARS results. a) Spectrum of the pump and probe pulse. The locations of the long pass (dashed) and short pass (solid) filters are also indicated. b) Time domain FTCARS signal for pyridine including the dominant CARS modes at 990 cm^{-1} and 1030 cm^{-1}, with smaller peaks at 983 cm^{-1} and 1070 cm^{-1}. The actual scan length was 12 ps, providing ~3 cm^{-1} resolution. c) CARS

view of the oscillatory FTCARS signal. The large signal at short delays arises from the nonresonant background generated by combined pump and probe pulses, and can be windowed out before obtaining the FTCARS spectrum, shown in Fig. 2(c). The spectral resolution of the measurement is determined by the maximum time delay, and in this case is

#72524 - $15.00 USD Received 30 June 2006; revised 21 August 2006; accepted 24 August 2006

~3 cm^{-1}. The combined pump and probe power used was 86 mW. The data acquisition time was 1.5 s, limited by the scanning speed of the stage, which could readily be increased.

To clarify the origin of the FTCARS signal, we plot the FTCARS signal as a function of the pump and probe intensity in Fig. 3, indicating a linear dependence on the pump intensity and a quadratic dependence on the probe intensity. This is consistent with the power dependence anticipated by Eq. (8). While the FTCARS signal is inherently homodyned by the resonant and nonresonant probe contributions, the current implementation lacks control over the amplification since the relative phase and intensity of the signal and local oscillator cannot be varied. By modifying the setup as shown in Fig. 1(d), version ii), the blue components of the probe spectrum can be used to provide the local oscillator (LO), and the relative phase and intensity of the signal and LO can be readily varied in a manner that we will call "controlled" FTCARS. In Fig. 4(a) we show the controlled and standard FTCARS spectra, demonstrating that control over the LO provides two orders of magnitude increase in CARS signal in the power spectrum. Other implementations of homodyne detection have been used to separate the resonant and nonresonant CARS contribution to obtain higher quality spectra that more closely match the Raman spectrum [30]. Here, controlled homodyne detection offers a signal enhancement, but does not change the information obtainable by the measurement: it is the ability to window out the early time domain data that reveals the CARS spectrum beneath the nonresonant background. Fig. 4(c) demonstrates our control over the homodyne amplification as the relative phase between the LO and the resonant and nonresonant CARS signals is varied. The phase variation was obtained by tilting the glass compensation plate in the probe arm. The enhanced signal provided by controlled homodyne detection permits much lower pump and probe power to be used. Fig. 5 shows the signal obtainable in a single scan with a pump power of 5 mW and a probe power of 5 mW. With the controlled homodyne method a lower probe power can be used because it is not necessary to rely on the probe to generate

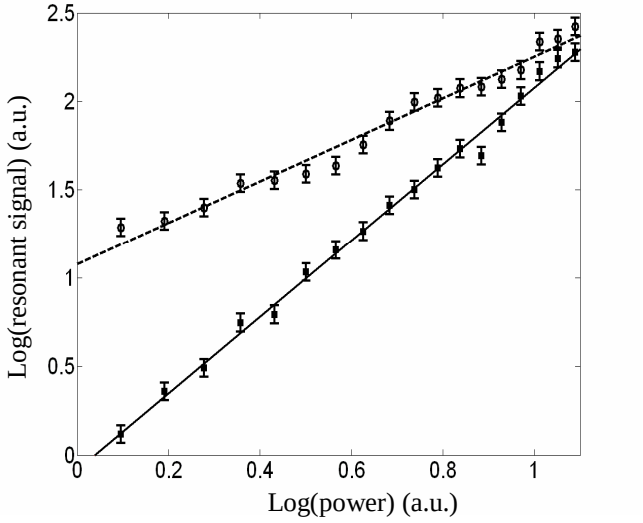

Fig. 3. Dependence of resonant CARS signal on the pump (dashed line) and probe (solid line) pulse power. Slopes of 1.18 and 2.16 indicate linear and quadratic dependence on the pump and probe power respectively. The resonant signal amplitude was measured from the CARS power spectrum. Simulations give slopes of 1 and 2 respectively.

#72524 - $15.00 USD Received 30 June 2006; revised 21 August 2006; accepted 24 August 2006

sufficient nonresonant and resonant CARS signals to act as the LO.

5. Discussion

High resolution CARS spectra spanning the fingerprint region are desirable in many microscopy applications, whether it be to obtain full spectrally resolved images, or for microspectroscopy applications where it is of interest to explore the chemistry of selected regions of a sample. Most CARS implementations have the ability to produce CARS spectra, either by scanning the pump-Stokes frequency difference, or by scanning a time delay. Others combine a narrowband pump and broadband probe to detect CARS spectra directly in the frequency domain. In all cases, obtaining a full spectrally resolved image is relatively slow. Many CARS implementations are limited in spectral resolution, or obtain improved spectral resolution at the expense of signal.

Being generated by nonlinear processes, both the resonant and nonresonant CARS and

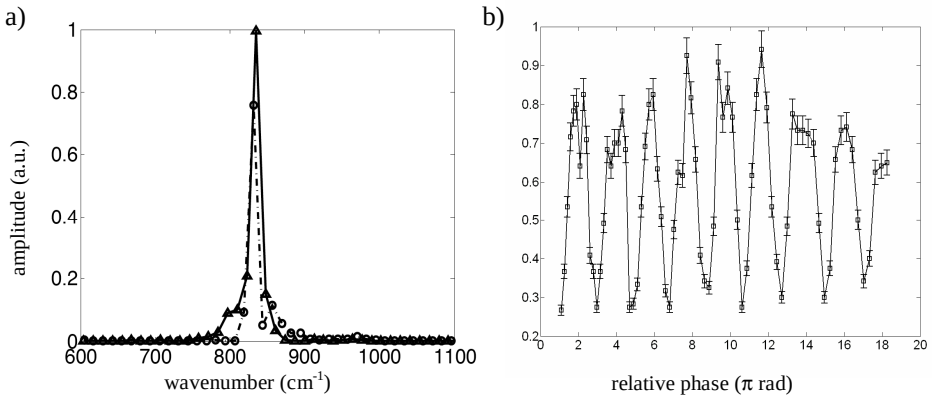

Fig. 4. (a). FTCARS power spectra obtained 2-propanol, exhibiting a single dominant peak near 820 cm^{-1}. The weak signal from regular detection (dashed line/circles) has been multiplied by 100 to appear visible on the same scale as the homodyne signal (solid line/triangles). b) Oscillation amplitude as a function of relative phase between the LO and the resonant and nonresonant FTCARS signals, demonstrating control over the homodyne amplification.

nonresonant background signals decrease when longer excitation pulses are used, with the nonresonant background decreasing more rapidly than the resonant signal [2]. For this reason, picosecond pulses have been used in the past, since they provide a balance between lower resonant signal and reduced nonresonant background. In FTCARS we have an effective method of removing the nonresonant background without the need to sacrifice resonant signal. Compared to picosecond CARS, FTCARS has the benefit of a simpler laser source: broadband Ti:sapphire oscillators are now commercially available, turnkey instruments. For acquiring spectra, scanning a time delay in FTCARS may be simpler than tuning the Stokes frequency as required by the picosecond method, in particular if two phase-locked lasers are employed. A disadvantage of the FTCARS technique is the relative difficulty of managing dispersion for ultrashort femtosecond pulses compared to picosecond pulses. Perhaps more limiting is the fact that FTCARS cannot selectively image a single CARS mode, which could be desirable in applications where detailed spectral information is not needed or rapid imaging is essential. This limitation could be overcome with coherent-control methods such as those already demonstrated [9]. In applications requiring rapid image acquisition it may be most practical to combine FTCARS with other faster imaging methods such as fluorescence to perform microspectroscopy in selected sample regions.

#72524 - $15.00 USD Received 30 June 2006; revised 21 August 2006; accepted 24 August 2006

While the FTCARS method is similar to phase-shaped CARS [9], it employs a simpler setup and can acquire spectra more rapidly than implementations employing liquid crystal spatial light modulators, which cannot rapidly change phase modulation as required for acquiring spectra. While this technical hurdle was recently overcome with a faster phase-modulation switching method [32], the spectral resolution of phase-shaped CARS remains limited by the complexity of the modulation that can be generated by the pulse-shaper. In contrast, FTCARS has essentially arbitrary spectral resolution determined by the maximum delay between pump and probe pulses. This is a distinct advantage over chirped-pulse CARS implementations, which "focus" the spectrum of broadband excitation to select a given CARS mode [15-17]. A CARS spectrum can be recorded by varying the time-delay between broadband, chirped, exciting pulses. Alternately, a recent implementation chirped only the pump pulse and used spectral interferometric detection to obtain broadband CARS spectra.[29] In these chirped-pulse CARS methods, the spectral resolution depends critically on the chirp, with greater chirp providing greater spectral resolution. Thus increased spectral resolution comes with the price of a diminished resonant CARS signal, as chirping reduces the peak excitation pulse intensity.

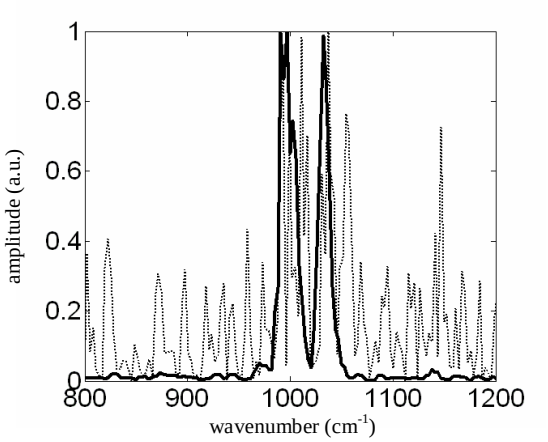

Fig. 5. Controlled homodyne (solid) and standard FTCARS (dashed) spectra of pyridine using 5mW pump and 5 mW probe power.

Compared to recent spectrally resolved CARS methods, which employ a narrow pump pulse and resolve the CARS signal in a spectrometer [13,14,18,20], FTCARS offers more efficient detection since lossy gratings are avoided and a single detector is used. The resonant FTCARS signals will also be higher since the peak excitation intensity is greater with impulsive rather than narrowband excitation. While scanning a time delay is not required in spectrally resolved configurations, the relatively low signal will require averaging of the weak signal and increase acquisition times.

6. Conclusion

We have discussed the origin of the FTCARS signal and demonstrated that it is an inherently homodyned signal arising from resonant CARS generated by the pump and probe interactions mixing with contributions coming solely from the probe pulse. We also demonstrated control over the homodyne signal by adding an additional LO field derived from the blue edge of the probe pulse. By interferometric control of the LO we achieved two orders of magnitude increase in resonant CARS signal. Compared to other implementations, FTCARS is based on a single broadband laser source, and is a straightforward spectroscopy that will prove useful in

#72524 - $15.00 USD Received 30 June 2006; revised 21 August 2006; accepted 24 August 2006

microscopy and microspectroscopy applications where high resolution CARS spectra are desired.

#72524 - $15.00 USD Received 30 June 2006; revised 21 August 2006; accepted 24 August 2006